# Gas transfer velocities of $CO_2$ in subtropical monsoonal climate streams and small rivers

**Siyue Li[a]*, Rong Mao[a], Yongmei Ma[a], Vedula V. S. S. Sarma[b]**

a. Chongqing Institute of Green and Intelligent Technology, Chinese Academy of Sciences, Chongqing 400714, China

b. CSIR-National Institute of Oceanography, Regional Centre, Visakhapatnam, India

**Correspondence**

**Siyue Li**

*Chongqing Institute of Green and Intelligent Technology (CIGIT),*

*Chinese Academy of Sciences (CAS).*

*266, Fangzheng Avenue, Shuitu High-tech Park, Beibei, Chongqing 400714, China.*

*Tel: +86 23 65935058; Fax: +86 23 65935000*

*Email: syli2006@163.com*

## Abstract

$CO_2$ outgassing from rivers is a critical component for evaluating riverine carbon cycle, but it is poorly quantified largely due to limited measurements and modeling of gas transfer velocity (k) in subtropical streams and rivers. We measured $CO_2$ flux rates, and calculated k and partial pressure ($pCO_2$) in 60 river networks of the Three Gorges Reservoir (TGR) region, a typical area in the upper Yangtze River with monsoonal climate and mountainous terrain. The observed determined $k_{600}$ values ($k_{600}$=48.4±53.2 cm/h) were showed large variability due to spatial variations in physical controls on surface water turbulence. Our flux-derived k values measurements using chambers were comparable with model derived from flow velocities. Unlike in open waters, k is more pertinent to flow velocity and water depth in the studied small river systems. Our results show that TGR river networks emitted approx. 1.4 Tg $CO_2$/y using varying approaches such as chambers, derivedmeasured k and developed k model. This study suggests that incorporating scale-appropriate k measurements into extensive $pCO_2$ investigation is required to refine basin-wide carbon budgets in the subtropical streams and small rivers. We concluded that simple parameterization of k as a function of morphological characteristics was site specific and hence highly variable in rivers of the upper Yangtze River. k models should be developed for stream studies to evaluate the contribution of these regions to atmospheric $CO_2$.

**Key words**: $CO_2$ outgassing, riverine C flux, flow velocity, physical controls, Three Gorge Reservoir, Yangtze River

带格式的: 下标

## 1. Introduction

Rivers serve as a significant contributor of $CO_2$ to the atmosphere (Cole *et al.*, 2007; Tranvik *et al.*, 2009; Li *et al.*, 2012; Raymond *et al.*, 2013). As a consequence, accurate quantification of riverine $CO_2$ emissions is a key component to estimate net continental carbon (C) flux (Raymond *et al.*, 2013). More detailed observational data and ~~new~~ accurate measurement techniques are critical to refine the riverine C budgets (Raymond and Cole, 2001; Li and Bush, 2015). Generally two methods are used to estimate $CO_2$ areal fluxes from the river system, such as direct measurements floating chambers (FCs), and indirect calculation of thin boundary layer (TBL) model that depends on gas concentration at air-water gradient and gas transfer velocity, k (Guerin *et al.*, 2007; Xiao *et al.*, 2014). Direct measurements are normally laborious, while the latter method shows ease and simplicity and thus is preferred (Butman and Raymond, 2011; Li *et al.*, 2012; Li *et al.*, 2013; Lauerwald *et al.*, 2015; Ran *et al.*, 2015).

The areal flux of $CO_2$ (F, unit in mmol/m$^2$/d) *via* the water–air interface by TBL is described as follows:

$$F = k \times K_h \times \triangle pCO_2 \qquad (1)$$

$$K_h = 10^{-(1.11 + 0.016 * T - 0.00007 * T^2)} \qquad (2)$$

where $k$ (unit in m/d) is the gas transfer velocity of $CO_2$ (also referred to as piston velocity) at the *in situ* temperature (Li *et al.*, 2016). $\triangle pCO_2$ (unit in µatm) is the air-water gradient of $pCO_2$ (Borges *et al.*, 2004). $K_h$ (mmol/m$^3$/ µatm) is the aqueous-phase solubility coefficient of $CO_2$ corrected using temperature ($T$ in ℃) (Li *et al.*, 2016).

△$pCO_2$ can be measured ~~precisely~~ well in various aquatic systems, however, the accuracy of the estimation of flux is depended on the k value. Broad ranges of k for $CO_2$ (Raymond and Cole, 2001; Borges *et al.*, 2004; Raymond *et al.*, 2012) were reported due to variations in techniques, tracers used and governing processes. k is controlled by turbulence at the surface aqueous boundary layer, hence, $k_{600}$ (the standardized gas transfer velocity at a temperature of 20 $^0$C) is parameterized as a function of wind speed in open water systems of reservoirs, lakes, and oceans (Borges *et al.*, 2004; Guerin *et al.*, 2007; Wanninkhof *et al.*, 2009). While in streams and small rivers, turbulence at the water-air interface is generated by shear stresses at streambed, thus k is modeled using channel slope, water depth, and water velocity in particular (Alin *et al.*, 2011; Raymond *et al.*, 2012). Variable formulations of k have been established by numerous theoretical, laboratory and field studies, nonetheless, better constraint on k levels is still required as its levels are very significant and specific due to large heterogeneity in hydrodynamics and physical characteristics of river networks. This highlights the importance of k measurements in a wide range of environments for the accurate upscaling of $CO_2$ evasion, and for parameterizing the physical controls on $k_{600}$. However, only few studies provide information of k for riverine $CO_2$ flux in Asia (Alin *et al.*, 2011; Ran *et al.*, 2015), and those studies do not address the variability of k in China's small rivers and streams.

Limited studies demonstrated that higher levels of k in the Chinese large rivers (Alin *et al.*, 2011; Ran *et al.*, 2015; Liu *et al.*, 2017; Ran *et al.*, 2017), which contributed to much higher $CO_2$ areal flux particularly in China's monsoonal rivers that are impacted by concentrated seasonal precipitationhydrological seasonality. The monsoonal flow pattern and thus flow velocity is expected to be different than other rivers in the world, as a consequence, k levels should be different than others, and potentially is higher in subtropical monsoonal rivers.

Considerable efforts, such as purposeful (Jean-Baptiste and Poisson, 2000; Crusius and Wanninkhof, 2003) and natural tracers (Wanninkhof, 1992) and FCs (Borges *et al.*, 2004; Guerin *et al.*, 2007; Alin *et al.*, 2011; Prytherch *et al.*, 2017), have been carried out to estimate accurate k values. The direct determination of k by FCs is more popular due to simplicity of the technique for short-term $CO_2$ flux measurements (Raymond and Cole, 2001; Xiao *et al.*, 2014; Prytherch *et al.*, 2017). Prior reports, however, have demonstrated that k values and the parameterization of k as a function of wind and/or flow velocity (probably water depth) vary widely across rivers and streams (Raymond and Cole, 2001; Raymond *et al.*, 2012). To contribute to this debate, extensive investigation was firstly accomplished for determination of k in rivers and streams of the upper Yangtze using FC method. Models of k were further developed using hydraulic properties by flux measurements and TBL model. Our new contributions to the literature includeare (1) providing first determination and controls of k levels for small rivers and streams in subtropical areas of China, and (2) comparisons of two methods for $CO_2$ areal fluxes by FCs and models developednew models developed in the subtropical mountainous river networks. The outcome of this study is expected to help in accurate estimation of $CO_2$ evasion from subtropical rivers and streams, and thus refine riverine C budget over a regional/basin scale.

Our recent study preliminarily investigated $pCO_2$ and air – water $CO_2$ areal flux as well as their controls from fluvial networks in the Three Gorges Reservoir (TGR) area (Li *et al.*, 2018). The past study was based on two field works, and the diffusive models from other continents were used. In this study, we attempted to derive k levels and develop the gas transfer model in this area (mountainous streams and small rivers) for more accurate quantification of $CO_2$ areal flux, and also to serve for the fluvial networks in the Yangtze River or others with similar hydrology and geomorphology. Moreover, we did detailed field campaigns in the two contrasting rivers Daning and Qijiang for models (Fig. 1). The study thus clearly stated distinct differences than the previous study (Li *et al.*, 2018) by the new contributions of specific objectives and data supplements, as well as wider significance.

## 2. Materials and methods

### 2.1. Study areas

All field measurements were carried out in the rivers and streams of the Three Gorges Reservoir (TGR) region (28°44′–31°40′N, 106°10′–111°10′E) that is locating in the upper Yangtze River, China (Fig. 1S1). This region is subject to humid subtropical monsoon climate with an average annual temperature ranging between15 and 19 ℃. Average annual precipitation is approx. 1250 mm with large intra- and inter-annual variability. About 75% of the annual total rainfall is concentrated in April through September (Li *et al.*, 2018).

The river sub-catchments include large scale river networks covering the majority of the tributaries of the Yangtze in the TGR region, i.e., 32 first-order tributaries and 16 second-order48 tributaries were collected. These tributaries have drainage areas that vary widely from 100 to 4400 km$^2$ with width ranging from 1 m to less than 100 m. The annual discharges from these tributaries have a broad spectrum of 1.8 – 112 m$^3$/s. Detailed samplings were conducted in the two largest rivers of Daning (35 sampling sites) and Qijiang (32 sites) in the TGR region. These two river basins drain catchment areas of 4200 and 4400 km$^2$-.with maximal third-order tributariesThe studied river systems had width < 100 m, we thus defined them as small rivers and streams. The Daning and Qijiang river systems are underlain by widely carbonate rock, and locating in a typical karst area. The location of sampling sites is deciphered in Fig. 1S1. The detailed information on sampling sites and primary data are presented in the Supplement Materials (Appendix Table A1). The sampling sites are outside the Reservoirs and are not affected by dam operation.

**2.2. Water sampling and analyses**

Three fieldwork campaigns from the main river networks in the TGR region were undertaken during May through August in 2016 (i.e., 18-22 May for Daning, 21 June-2 July for the entire tributaries of TGR, and 15-18 August for Qijiang). A total of 115 discrete grab samples were collected (each sample consistededs of three replicates). Running waters were taken using pre acid-washed 5-L high density polyethylene (HDPE) plastic containers from depths of 10 cm below surface. The samples were filtered through pre-baked Whatman GF/F (0.7-μm pore size) filters on the sampling day and immediately stored in acid-washed HDPE bottles. The bottles were transported in ice box to the laboratory and stored at 4 ℃ for analysis. Concentrations of dissolved organic carbon (DOC), dissolved total nitrogen (DTN), and dissolved total phosphorus (DTP) were determined within 7 days of water collection (Mao *et al.*, 2017).

Water temperature (T), *p*H, DO saturation (DO%) and electrical conductivity (EC) were measured *in situ* by the calibrated multi-parameter sondes (HQ40d HACH, USA, and YSI 6600, YSI incorporated, USA). pH, the key parameter for $pCO_2$ calculation, was measured to a precision of ±0.002, and pH sonde wasis calibrated by the certified reference materials (CRMs) before measurements with an accuracy is better than 0.2%. Atmospheric $CO_2$ concentrations were determined *in situ* using PP Systems EGM-4 (Environmental Gas Monitor; PP SYSTEMS Corporation, USA). Total alkalinity was measured using a fixed endpoint titration method with 0.0200 mol/L hydrochloric acid (HCl) on the sampling day. DOC concentration was measured using a total organic carbon analyzer (TOC-5000, Shimadzu, Japan) with a precision better than 3% (Mao *et al.*, 2017). DTN and DTP concentrations were determined using a continuous-flow autoanalyzer (AA3, Seal Analytical, Germany) and/or spectrophotometer following peroxodisulfate oxidation (Ebina *et al.*, 1983). All the solvents and reagents used in experiments were of aAnalytical--reagent grade.- chemical were used for all experiments.

Concomitant stream width, depth and flow velocity were determined along the cross section. Wind speed at 1 m over the water surface ($U_1$) and air temperature (Ta) were measured with a Testo 410-1 handheld anemometer (Germany). Wind speed at 10 m height ($U_{10}$, unit in m/s) was calculated using the following formula (Crusius and Wanninkhof, 2003):

$$U_{10} = U_Z \left[ 1 + \frac{(C_{d10})^{1/2}}{K} \times \ln\left(\frac{10}{z}\right) \right] \quad (3)$$

where $C_{d10}$ is the drag coefficient at 10 m height (0.0013 m/s), and K is the von Karman constant (0.41), and z is the height (m) of wind speed measurement. The relationship was yielded when z=1 ($U_{10}$=1.208×$U_1$ as we measured the wind speed at a height of 1m ($U_1$)).

带格式的: 下标

Aqueous $pCO_2$ was computed from the measurements of pH, total alkalinity, and water temperature using $CO_2$ system ($k_1$ and $k_2$ are from Millero, 1979) (Lewis *et al.*, 1998), which have been identified as high quality data (Borges *et al.*, 2004; Li *et al.*, 2012; Li *et al.*, 2013).

## 2.3. Water-to-air $CO_2$ fluxes using FC method

FCs (30 cm in diameter, 30 cm in height) were deployed to measure air-water $CO_2$ fluxes and transfer velocities. They were made of cylindrical polyvinyl chloride (PVC) pipe with a volume of 21.20 L and a surface area of 0.071 $m^2$. These non-transparent, thermally insulated vertical tubes, covered by aluminum foil, were connected *via* $CO_2$ impermeable rubber-polymer tubing (with outer and inner diameters of 0.5 cm and 0.35 cm, respectively) to a portable non-dispersive infrared

$CO_2$ analyzer EGM-4 (PPSystems). Air was circulated through the EGM-4 instrument *via* an air filter using an integral ~~DC~~ pump at a flow rate of 350 ml/min. The chamber method was widely used and more details of advantages and limits on chambers were reviewed elsewhere (Borges *et al.*, 2004; Alin *et al.*, 2011; Xiao *et al.*, 2014).

Chamber measurements were conducted by deploying two replicate chambers or one chamber for two times at each site. In sampling sites with low and favorable flow conditions (Fig. S1), freely drifting chambers (DCs) were executed, while sampling sites in rivers and streams with higher flow velocity were conducted with anchored chambers (ACs) (Ran *et al.*, 2017). ACs would create overestimation of $CO_2$ emissions in our studied region (Lorke *et al.*, 2015). Data were logged automatically and continuously at 1-min interval over a given span of time (normally 5-10 minutes) after enclosure. The $CO_2$ area flux (mg/m$^2$/h) was calculated using the following formula.

$$F = 60 \times \frac{dpco2 \times M \times P \times T_0}{dt \times V_0 \times P_0 \times T} H \qquad (4)$$

Where d$pco_2$/dt is the rate of concentration change in FCs (μl/l/min); M is the molar mass of $CO_2$ (g/mol); P is the atmosphere pressure of the sampling site (Pa); T is the chamber absolute temperature of the sampling time (K); $V_0$, $P_0$, $T_0$ is the molar volume (22.4 l/mol), $P_0$ is atmosphere pressure (101325 Pa), and $T_0$ is absolute temperature (273.15 K) –under the standard condition; H is the chamber height above the water surface (m) (Alin *et al.*, 2011). We accepted the flux data that had a good linear regression of flux against time ($R^2 \geq 0.95$, $p<0.01$) following manufacturer' specification. In our sampling points, all measured fluxes were retained since the

**带格式的:** Default, 缩进: 首行缩进: 2 字符, 定义网格后自动调整右缩进, 调整中文与西文文字的间距, 调整中文与数字的间距

floating chambers yielded linearly increasing $CO_2$ against time.

Water samples from a total of 115 sites were collected. Floating chambers with replicates were deployed in 101 sites (32 sampling sites in Daning, 37 sites in TGR river networks and 32 sites in Qijiang). The sampling period covered spring and summer season, our sampling points are reasonable considering a water area of 433 $km^2$. For example, 16 sites were collected for Yangtze system to examine hydrological and geomorphological controls on *p*$CO_2$ (Liu *et al.*, 2017), and 17 sites for dynamic biogeochemical controls on riverine *p*$CO_2$ in the Yangtze basin (Liu *et al.*, 2016). Similar to other studies, sampling and flux measurements in the day would tend to underestimate $CO_2$ evasion rate (Bodmer *et al.*, 2016).

带格式的：下标

**2.4. Calculations of the gas transfer velocity**

The k was ~~computed with~~calculated by reorganizing ~~E~~eq (1). To make comparisons, k is normalized to a Schmidt (Sc) number of 600 ($k_{600}$) at a temperature of 20 ℃.

$$k_{600} = k_T \left(\frac{600}{S_{CT}}\right)^{-0.5} \qquad (5)$$

$$S_{CT} = 1911.1 - 118.11T + 3.4527T^2 - 0.04132T^3 \qquad (5)$$

Where $k_T$ is the measured values at the *in situ* temperature (T, unit in $^{o}$C), $S_{CT}$ is the Schmidt number of temperature T. Dependency of ~~k proportional to $Sc^{-0.5}$~~ -0.5 was employed here as measurement were made in ~~highly~~ turbulent rivers and streams in this study (Wanninkhof, 1992; Borges *et al.*, 2004; Alin *et al.*, 2011).

**2.5. Estimation of river water area**

Water surface is an important parameter for $CO_2$ efflux estimation, while it depends on its climate, channel geometry and topography. River water area therefore largely fluctuates with much higher areal extent of water surface particularly in monsoonal season. However, most studies do not consider this change, and a fraction of the drainage area is used in river water area calculation (Zhang *et al.*, 2017). In our study, a 90 m resolution SRTM DEM (Shuttle Radar Topography Mission digital elevation model) data and Landsat images in dry season were used to delineate river network, and thus water area (Zhang *et al.*, 2018), whilst, stream orders were not extracted. Water area of river systems is generally much higher in monsoonal season in comparison to dry season, for instance, Yellow River showed 1.4-fold higher water area in the wet season than in the dry season (Ran *et al.*, 2015). Available dry-season image was likely to underestimate $CO_2$ estimation.

带格式的: 下标

**2.65. Data processing**

Prior to statistical analysis, we excluded $k_{600}$ data for samples with the air-water $pCO_2$ gradient <110 μatm, since the error in the $k_{600}$ calculations drastically enhances when $\Delta pCO_2$ approaches zero (Borges *et al.*, 2004; Alin *et al.*, 2011),. and datasets with $\Delta pCO_2$ >110 μatm provide an error of <10% on $k_{600}$ computation. Thus, we discarded the samples (36.7% of sampling points with flux measurements) with $\Delta pCO_2$ <110 μatm for $k_{600}$ model development, while for the flux estimations from diffusive model and floating chambers, all samples were included.

Spatial differences (Daning, Qijiang and entire tributaries of TGR region) were tested using the nonparametric Mann Whitney U-test. Multivariate statistics, such as correlation and stepwise multiple linear regression, were performed for the models of $k_{600}$ using potential physical parameters, such as of wind speed, water depth, and current velocity as the independent variables from both separated data and combined data (Alin *et al.*, 2011). k models were obtained by water depth using data from the TGR rivers, while by flow velocity in the Qijiang. All statistical relationships were significant at $p < 0.05$. The statistical processes were conducted using SigmaPlot 11.0 and SPSS 16.0 for Windows (Li *et al.*, 2009; Li *et al.*, 2016).

## 3. Results

### 3.1. $CO_2$ partial pressure and key water quality variables

The significant spatial variations in water temperature, pH, $pCO_2$, DOC and nutrients (DTN and DTP) were observed among Daning, TGR and Qijiang rivers whereas alkalinity did not display such variability (Fig. S2). *p*H varied from 7.47 to 8.76 9.38 (mean of 8.39 ±0.29) with exceptions of two quite high values of 9.38 and 8.87 (mean: 8.39 ±0.29 from total dataset). and Much lower *p*H was observed in TGR rivers (8.21 ±0.33) (Table 1; $p<0.05$; Fig. S2). $pCO_2$ varied between 50 and 4830 µatm with mean of 846 ±819 µatm (Table 1). There were 28.7% of samples that had $pCO_2$ levels lower than 410 µatm, , suggesting that all threewhile the studied rivers wereare overall supersaturated with reference to atmospheric $CO_2$ and act as a source for the atmospheric $CO_2$. The $pCO_2$ levels were 2.1 to 2.6-fold higher in TGR rivers than Daning (483 ±294 µatm) and Qijiang Rivers (614 ±316 µatm) (Fig. S2). The calculated $pCO_2$ levels were within the published range, but towards the lower-end of published concentrations compiled elsewhere (Cole and Caraco, 2001; Li *et al.*, 2013). The total mean $pCO_2$ (846 μatm) in the TGR, Danning and Qijiang sampled is lower than one third of global river's average (3220 μatm) (Cole and Caraco, 2001).

域代码已更改

The much higher concentrations of dissolved organic carbon (DOC) and dissolved nutrients (DTN and DTP) (Fig. S3) were observed in the TGR rivers ($p<0.01$ by Mann-Whitney Rank Sum Test; Fig. S3) than Qijang and Danning. In comparison to Daning, Qijiang showed significantlyRelatively higher concentrations of DOC and DTN ($p<0.05$), and much lower– were observed in Qijang than Daning River but mean TDP concentrationwas much higher in latter than former river ($p<0.05$; Fig. S3; Table 1).

带格式的: 字体: (默认) Times New Roman, 小四, 非加粗

**3.2. $CO_2$ flux using floating chambers**

The calculated $CO_2$ areal fluxes were higher in TGR rivers (217.7 ± 334.7 mmol/m$^2$/d, n = 35), followed by Daning (122.0 ± 239.4 mmol/m$^2$/d, n = 28) and Qijiang rivers (50.3 ± 177.2 mmol/m$^2$/d, n = 32) (Fig. 21). The higher $CO_2$ evasion from the TGR rivers is consistent with high riverine $pCO_2$ levels. The mean $CO_2$ emission rate was 133.1 ± 269.1 mmol/m$^2$/d (n = 95) in all three rivers sampled. The mean $CO_2$ flux differed significantly between TGR rivers and Qijiang (Fig. 21). The ratio of mean to median of $CO_2$ areal flux ranged between 1.4 (Qijiang) and 2.6 (TGR rivers).

### 3.3. k levels

~~Samples with $\Delta pCO_2$ less than 110 µatm were excluded for $k_{600}$ calculations, thus a~~ A total of 64 data were used (10 for Daning River, 33 for TGR rivers and 21 for Qijiang River) to develop k model after removal of samples with $\Delta pCO_2$ less than 110 µatm (Table 2). No significant variability in $k_{600}$ values were observed among the three rivers sampled (Fig. 3~~2~~). The mean $k_{600}$ (unit in cm/h) was~~is~~ relatively higher in Qijiang (60.2 ±78.9), followed by Daning (50.2 ±20.1) and TGR rivers (40.4 ±37.6), while the median $k_{600}$ (unit in cm/h) was higher in Daning (50.5), followed by TGR rivers (30.0) and Qijiang (25.8) (Fig. 3~~2~~; Table S1). Combined ~~Binned~~ $k_{600}$ data were averaged to 48.4 ±53.2 cm/h (95% CI: 35.1-61.7), and it is 1.5-fold higher than the median value (32.2 cm/h) (Fig. 3~~2~~).

带格式的：下标

## 4. Discussion

### 4.1. Determined k values relative to world rivers

带格式的

We derived first-time the k values in the subtropical streams and small rivers. Our determined~~measured~~ $k_{600}$ levels with a 95% CI of 35.1 to 61.7 (mean: 48.4) cm/h is compared well with a compilation of data for streams and small rivers (e.g., 3-70 cm/h) (Raymond *et al.*, 2012). Our determined $k_{600}$ values are greater than the global rivers' average (8 - 33 cm/h) (Butman and Raymond, 2011; Raymond *et al.*, 2013), and much higher than mean for tropical and temperate large rivers (5-31 cm/h) (Alin *et al.*, 2011). These studies evidences that $k_{600}$ values are highly variable in streams

带格式的：下标

and small rivers (Alin *et al.*, 2011; Ran *et al.*, 2015). Though the mean $k_{600}$ in the TGR, Daning and Qijiang is higher than global mean, however, it is consistent with $k_{600}$ values in the main stream and river networks of the turbulent Yellow River (42 ± 17 cm/h) (Ran *et al.*, 2015), and Yangtze (38 ±40 cm/h) (Liu *et al.*, 2017) (Table S2).

The calculated $pCO_2$ levels were within the published range, but towards the lower-end of published concentrations compiled elsewhere (Cole and Caraco, 2001; Li *et al.*, 2013). The total mean $pCO_2$ (846 ±819 μatm) in the TGR, Danning and Qijiang sampled was~~is~~ lower than one third of global river's average (3220 μatm) (Cole and Caraco, 2001). The lower $pCO_2$ than most of the world's river systems, particularly the under-saturated values, demonstrated that heterotrophic respiration of terrestrially derived DOC was not significant. Compared with high alkalinity, the limited delivery DOC particularly in the Daning and Qijiang river systems (Figs. S2 and S3) also indicated that in-stream respiration was limited. These two river systems are characterized by karst terrain and underlain by carbonate rock, where photosynthetic uptake of dissolved $CO_2$ and carbonate minerals dissolution considerably regulated aquatic $pCO_2$ (Zhang *et al.*, 2017).

Higher pH levels were observed in Daning and Qijiang river systems ($p<0.05$ by Mann-Whitney Rank Sum Test), where more carbonate rock exists that are characterized by karst terrain. Our pH range was comparable to the recent study on the karst river in China (Zhang *et al.*, 2017). Quite high values (i.e., 9.38 and 8.87) were recorded in some investigated sites, where chemical enhancement would increase the influx of atmospheric $CO_2$ to alkaline waters (Wanninkhof and Knox,

带格式的：下标

带格式的：下标

域代码已更改

带格式的：字体：(默认) Times New Roman，非突出显示

带格式的：下标

带格式的：定义网格后自动调整右缩进，调整中文与西文文字的间距，调整中文与数字的间距

1996), while 1.7% of sampling sites that were strongly affected by chemical enhancement were not significant on a regional scale. This chemical enhancement of $CO_2$ influx was also reported to be limited in high-pH rivers (Zhang *et al.*, 2017).

## **4.2. Hydraulic controls of $k_{600}$**

It has been well established that $k_{600}$ is governed by a multitude of physical factors particularly current velocity, wind speed, stream slope and water depth, of which, wind speed is the dominant factor of k in open waters such as large rivers and estuaries (Raymond and Cole, 2001; Crusius and Wanninkhof, 2003; Borges *et al.*, 2004; Alin *et al.*, 2011). In contrast $k_{600}$ in small rivers and streams is closely linked to flow velocity, water depth and channel slope (Alin *et al.*, 2011; Raymond *et al.*, 2012). Several studies reported that the combined contribution of flow velocity and wind speed to k is significant in the large rivers (Beaulieu *et al.*, 2012; Ran *et al.*, 2015). Thus, $k_{600}$ values are higher in the Yellow River (ca. 0-120 cm/h) as compared to the low-gradient River Mekong (0-60 cm/h) (Alin *et al.*, 2011; Ran *et al.*, 2015), due to higher ~~wind speed and~~ flow velocity in the Yellow River (1.8 m/s) than Mekong river (0.9±0.4 m/s), resulting in greater surface turbulence and higher $k_{600}$ level in the Yellow (42 ±17 cm/h) than Mekong river (15 ±9 cm/h). This could substantiate the higher $k_{600}$ levels and spatial changes in $k_{600}$ values of our three river systems. For instance, similar to other turbulent rivers in China (Ran *et al.*, 2015; Ran *et al.*, 2017), ~~The~~ high~~er~~ $k_{600}$ values in the TGR, Daning and Qjiang rivers were~~are~~ due to mountainous terrain catchment, high current velocity (10 – 150 cm/s) (Fig. ~~4~~3b),

带格式的: 字体: (默认) Times New Roman

带格式的: 缩进: 首行缩进: 0 厘米

带格式的: 下标

带格式的: 下标

带格式的: 下标

带格式的: 下标

带格式的: 下标

带格式的: 下标

带格式的: 下标

带格式的: 下标

bottom roughness, and shallow water depth (10 - 150 cm) (Fig. 43a). It has been suggested that shallow water enhances bottom shear, and the resultant turbulence increases k values (Alin *et al.*, 2011; Raymond *et al.*, 2012). These physical controls are highly variable across environmental types (Figs. 43a and 43b), hence, k values are expected to vary widely (Fig. 32). The $k_{600}$ values in the TGR rivers showed wider range (1-177 cm/h; Fig. 32; Table S1), spanning more than 2 orders of magnitude across the region, and it is consistent with the considerable variability in the physical processes on water turbulence across environmental settings. Similar broad range of $k_{600}$ levels was also observed in the China's Yellow basin (ca. 0-123 cm/h) (Ran *et al.*, 2015; Ran *et al.*, 2017).

Contrary to our expectations, no significant relationship was observed between $k_{600}$ and water depth, and current velocity using the entire data in the three (TGR, Danning and Qjiang) river systems (Fig. S45). There were not statistically significant relationships between $k_{600}$ and wind speed using separated data or combined data, and it is consistent with earlier studies (Alin *et al.*, 2011; Raymond *et al.*, 2012). Flow velocity showed linear relation with $k_{600}$, and the extremely high value of $k_{600}$ was observed during the periods of higher flow velocity (Fig. S45a) using combined data. Similar trend was also observed between water depth and $k_{600}$ values (Fig. S45b). The lack of strong correlation between $k_{600}$ and physical factors are probably due to combined effect of both flow velocity and water depth, as well as large diversity of channel morphology, both across and within river networks in the entire catchment (60, 000 km$^2$). This is further collaborated by weak correlations between $k_{600}$ and flow

带格式的：下标
带格式的：下标
带格式的：下标
带格式的：下标
带格式的：下标
带格式的：下标

velocity in the TGR rivers (Fig. 4~~3~~), where one or two samples were taken for a large scale examination. $k_{600}$ as a function of water depth was obtained in the TGR rivers, but it explained only 30% of the variance in $k_{600}$. However, model using data from Qijiang could explain 68% of the variance in $k_{600}$ (Fig. 4~~3~~b), and it was in line with general theory. Nonetheless, $k_{600}$ from our flow velocity based model (Fig. 4~~3~~b) ~~is~~ was potentially largely overestimated with consideration of other measurements (Alin *et al.*, 2015; Ran *et al.*, 2015; Ran *et al.*, 2017). When several extremely values ~~are~~ were removed, $k_{600}$ (cm/h) ~~is~~ was parameterized as follows ($k_{600}$ = 62.879FV + 6.8357, $R^2$= 0.52, p=0.019, FV-flow velocity with a unit of m/s), and this revised model ~~is~~ was in good agreement with the model in the river networks of the Yellow River (Ran *et al.*, 2017), but much lower than the model developed in the Yangtze system (Liu *et al.*, 2017) (Fig. 4~~3~~c). This ~~is~~ was reasonable because of $k_{600}$ values in the Yangtze system ~~are~~ were from large rivers with higher turbulence than Yellow and our studied rivers. Furthermore, the ~~measured~~ determined $k_{600}$ using FCs was, on average, consistent with the revised model (Table 2). These differences in relationship between spatial changes in $k_{600}$ values and physical characteristics further corroborated heterogeneity of channel geomorphology and hydraulic conditions across the investigated rivers.

The subtropical streams and small rivers are biologically more active and are recognized to exert higher $CO_2$ areal flux to the atmosphere, however, their contribution to riverine carbon cycling is still poorly quantified because of data paucity and the absence of k in particular. Larger uncertainty of riverine $CO_2$ emission

带格式的: 下标

带格式的: 下标

带格式的: 下标

带格式的: 下标

in China was anticipated by use of $k_{600}$ from other continents or climate zones. For instance, $k_{600}$ for $CO_2$ emission from tributaries in the Yellow River and karst rivers was originated from the model in the Mekong (Zhang *et al.*, 2017), and Pearl (Yao *et al.*, 2007), Longchuan (Li *et al.*, 2012), and Metropolitan rivers (Wang *et al.*, 2017), which are mostly from temperate regions. Our $k_{600}$ values will therefore largely improve the estimation of $CO_2$ evasion from subtropical streams and small rivers, and improve to refine riverine carbon budget. More studies, however, are clearly needed to build the model, based on flow velocity and slope/water depth given the difficulty in k quantification on a large scale.

带格式的：下标

## 4.3. Implications for large scale estimation

We compared $CO_2$ areal flux by FCs and models developed here (Fig. 43) and other studies (Alin *et al.*, 2011) (Tables 2 and 3). $CO_2$ evasion was estimated for rivers in China with k values ranged between 8 and 15 cm/h (Yao *et al.*, 2007; Wang *et al.*, 2011; Li *et al.*, 2012) (Table S2). These estimates of $CO_2$ evasion rate were considerably lower than using present $k_{600}$ values (48.4±53.2 cm/h). For instance, $CO_2$ emission rates in the Longchuan River (e.g., k=8 cm/h) and Pearl River tributaries (e.g., k=8-15 cm/h) were 3 to 6 times higher using present k values compared to earlier. We found that the determined $k_{600}$ average was marginally beyond the levels from water depth based model and the model developed by Alin et al (Alin *et al.*, 2011), while equivalent to the flow velocity based revised model, resulting in similar patterns of $CO_2$ emission rates (Table 2). Hence selection of k values would

带格式的：下标

significantly hamper the accuracy of the flux estimation. Therefore k must be estimated along with $pCO_2$ measurements to accurate flux estimations.

We used our measured $CO_2$ emission rates by FCs for upscaling flux estimates and it was found to be 1.39 Tg$CO_2$/y for all rivers sampled in our study (Table 3a). The estimated emission was close to that of the revised model (1.40 ±1.31 (95% confidence interval: 0.91-1.87) Tg $CO_2$/y), and using the determined k average, i.e., 1.37 ±1.28 (95% confidence interval: 0.89-1.84) Tg $CO_2$/y, but slightly higher than the estimation using water-depth based model (1.08 ±1.01 Tg $CO_2$/y) and Alin's model (1.06 ±1.00 Tg $CO_2$/y) (Table 3b). The estimate was within the range of our earlier work using TBL on the TGR river networks (0.64-2.33 Tg $CO_2$/y) (Li *et al.*, 2018). The higher emission, i.e., 3.29 ±3.08 (2.15-4.43) Tg $CO_2$/y, using flow velocity based model may be over-estimated (Table 3b). Therefore, this study suggests that $CO_2$ emissions from rivers and streams in this area may be underestimated, i.e., 0.03 Tg $CO_2$/y (Li *et al.*, 2017) and 0.37-0.44 Tg $CO_2$/y (Yang *et al.*, 2013) as the former used TBL model with a lower k level, and the latter employed floating chambers, but they both sampled very limited tributaries (i.e., 2-3 rivers). Therefore, measurements of k must be made mandatory along with pCO2 measurement in the river and stream studies.

## 4.4. Uncertainty assessment of $pCO_2$ and flux-derived $k_{600}$ values

带格式的：下标

The uncertainty of flux-derived k values mainly stem from $\Delta pCO_2$ (unit in ppm) and flux measurements (Lorke *et al.*, 2015; Bodmer *et al.*, 2016; Golub *et al.*, 2017).

Thus we provided uncertainty assessments caused by dominant sources of uncertainty from measurements of aquatic *p*$CO_2$ and $CO_2$ areal flux since uncertainty of atmospheric $CO_2$ measurement could be neglected.

In our study, aquatic *p*$CO_2$ was computed based on pH, alkalinity and water temperature rather than directly measured. Recent studies highlighted *p*$CO_2$ uncertainty caused by systematic errors over empiric random errors (Golub *et al.*, 2017). Systematic errors are mainly attributed to instrument limitations, i.e., sondes of pH and water temperature. The relative accuracy of temperature meters was ±0.1 $^{0}$C according to manufacturers' specifications, thus the uncertainty of water T propagated on uncertainty in *p*$CO_2$ was minor (Golub *et al.*, 2017). Systematic errors therefore stem from pH, which has been proved to be a key parameter for biased *p*$CO_2$ estimation calculated from aquatic carbon system (Li *et al.*, 2013; Abril *et al.*, 2015). We used a high accuracy of pH electrode and the pH meters were carefully calibrated using CRMs, and *in situ* measurements showed an uncertainty of ±0.01. We then run an uncertainty of ±0.01 pH to quantify the *p*$CO_2$ uncertainty, and an uncertainty of ±3% was observed. Systematic errors thus seemed to show little effects on *p*$CO_2$ errors in our study.

Random errors are from repeatability of carbonate measurements. Two replicates for each sample showed the uncertainty of within ±5%, indicating that uncertainty in *p*$CO_2$ calculation from alkalinity measurements could be minor.

The measured pH ranges also exhibited great effects on *p*$CO_2$ uncertainty (Hunt *et al.*, 2011; Abril *et al.*, 2015). At low pH, p$CO_2$ can be overestimated when

**带格式的:** 字体：小四，倾斜，字体颜色：黑色

calculated from pH and alkalinity (Abril *et al.*, 2015). Samples for $CO_2$ fluxes estimated from pH and alkalinity showed pH average of 8.39 ±0.29 (median 8.46 with quartiles of 8.24-8.56) (n=115). Thus, overestimation of calculated $CO_2$ areal flux from pH and alkalinity is likely to be minor. Further, contribution of organic matter to non-carbonate alkalinity is likely to be neglected because of low DOC (mean 6.67 mg/L; median 2.51 mg/L) (Hunt *et al.*, 2011; Li *et al.*, 2013).

Recent study reported fundamental differences in $CO_2$ emission rates between ACs and freely DFs (Lorke *et al.*, 2015), i.e., ACs biased the gas areal flux higher. However, some studies observed that ACs showed reasonable agreement with other flux measurement techniques (Galfalk *et al.*, 2013), and this straightforward, inexpensive and relatively simple method AC was widely used (Ran *et al.*, 2017) Water-air interface $CO_2$ flux measurements were primarily made using ACs in our studied streams and small rivers because of relatively high current velocity; otherwise, floating chambers will travel far during the measurement period. In addition, inflatable rings were used for sealing the chamber headspace and submergence of ACs was minimal, therefore, our measurements were potentially overestimated but reasonable.

Sampling seasonality considerably regulated riverine $pCO_2$ and gas transfer velocity and thus water-air interface $CO_2$ evasion rate (Li *et al.*, 2012; Ran *et al.*, 2015). We sampled waters in wet season due to that it showed wider range of flow velocity and thus it covered the $k_{600}$ levels in the whole hydrological season. Wet season generally had higher current velocity and thus higher gas transfer velocity

**带格式的:** 首行缩进： 2 字符，定义网格后不调整右缩进，不调整西文与中文之间的空格，不调整中文和数字之间的空格

**带格式的:** 下标

(Ran *et al.*, 2015), while aquatic $pCO_2$ was variable with seasonality. We recently reported that riverine $pCO_2$ in the wet season was 81% the level in the dry season (Li *et al.*, 2018), and prior study on the Yellow River reported that k level in the wet season was 1.8-fold higher than in the dry season (Ran *et al.*, 2015), while another study on the Wuding River demonstrated that k level in the wet season was 83%-130% of that in the dry season (Ran *et al.*, 2017). Thus, we acknowledged a certain amount of errors on the annual flux estimation from one-time sampling campaign during the wet season in the TGR area, while this uncertainty could not be significant because that the diluted $pCO_2$ could alleviate the potentially increased k level in the wet season.

**5. Conclusion**

We provided first determination of gas transfer velocity (k) in the subtropical streams and small rivers. High variability in k values (mean 48.4 ± 53.2 cm/h) was observed, reflecting the variability of morphological characteristics on water turbulence both within and across river networks. The determined k using floating chambers (FCs) was comparable to our newly water depth based model, while substantially lower than flow velocity based model. We highlighted that k estimate from empirical model should be pursued with caution and the significance of incorporating k measurements along with extensive $pCO_2$ investigation is highly essential for upscaling to watershed/regional scale carbon (C) budget.

Riverine $pCO_2$ and $CO_2$ areal flux showed pronounced spatial variability with much higher levels in the TGR rivers. The $CO_2$ areal flux was averaged at 133.1 ± 269.1 mmol/m$^2$/d using FCs, the resulting emission was around 1.39 Tg $CO_2$/y, similar to the scaling up emission with the determined k, and the revised flow velocity based model, while marginally above the water depth based model. More work is clearly needed to refine the k modeling in the river systems of the upper Yangtze River for evaluating regional C budgets.

## Acknowledgements

This study was funded by "the Hundred-Talent Program" of the Chinese Academy of Sciences (R53A362Z10; granted to Dr. Li), and the National Natural Science Foundation of China (Grant No. 31670473). We are grateful to Mrs. Maofei Ni and Tianyang Li, and Miss Jing Zhang for their assistance in the field works. Users can access the original data from an Appendix. Special thanks are given to editor and anonymous reviewers for improving the Ms.

## References


Abril, G., Bouillon, S., Darchambeau, F., Teodoru, C.R., Marwick, T.R., Tamooh, F., Omengo, F.O., Geeraert, N., Deirmendjian, L., Polsenaere, P., Borges, A.V., 2015. Technical Note: Large overestimation of pCO(2) calculated from pH and alkalinity in acidic, organic-rich freshwaters. Biogeosciences 12, 67-78.

Alin, S.R., Maria, D.F.F.L.R., Salimon, C.I., Richey, J.E., Holtgrieve, G.W., Krusche, A.V., Snidvongs, A., 2015. Physical controls on carbon dioxide transfer velocity and flux in low - gradient river systems and implications for regional carbon budgets. Journal of Geophysical Research Biogeosciences 116, 248-255.

Alin, S.R., Rasera, M., Salimon, C.I., Richey, J.E., Holtgrieve, G.W., Krusche, A.V., Snidvongs, A., 2011. Physical controls on carbon dioxide transfer velocity and flux in low-gradient river systems and implications for regional carbon budgets. Journal of Geophysical Research-Biogeosciences 116.

Beaulieu, J.J., Shuster, W.D., Rebholz, J.A., 2012. Controls on gas transfer velocities in a large river. Journal of Geophysical Research-Biogeosciences 117.

Bodmer, P., Heinz, M., Pusch, M., Singer, G., Premke, K., 2016. Carbon dynamics and their link to dissolved organic matter quality across contrasting stream ecosystems. Science of the Total Environment 553, 574-586.

Borges, A.V., Delille, B., Schiettecatte, L.S., Gazeau, F., Abril, G., Frankignoulle, M., 2004. Gas transfer velocities of CO2 in three European estuaries (Randers Fjord, Scheldt, and Thames). Limnology and Oceanography 49, 1630-1641.

Butman, D., Raymond, P.A., 2011. Significant efflux of carbon dioxide from streams and rivers in the United States. Nature Geoscience 4, 839-842.

Cole, J.J., Caraco, N.F., 2001. Carbon in catchments: connecting terrestrial carbon losses with aquatic metabolism. Marine and Freshwater Research 52, 101-110.

Cole, J.J., Prairie, Y.T., Caraco, N.F., McDowell, W.H., Tranvik, L.J., Striegl, R.G., Duarte, C.M., Kortelainen, P., Downing, J.A., Middelburg, J.J., Melack, J., 2007. Plumbing the Global Carbon Cycle: Integrating Inland Waters into the Terrestrial Carbon Budget. Ecosystems 10, 172-185.

Crusius, J., Wanninkhof, R., 2003. Gas transfer velocities measured at low wind speed over a lake. Limnology and Oceanography 48, 1010-1017.

Ebina, J., Tsutsui, T., Shirai, T., 1983. SIMULTANEOUS DETERMINATION OF TOTAL NITROGEN AND TOTAL PHOSPHORUS IN WATER USING PEROXODISULFATE OXIDATION. Water Research 17, 1721-1726.

Galfalk, M., Bastviken, D., Fredriksson, S.T., Arneborg, L., 2013. Determination of the piston velocity for water-air interfaces using flux chambers, acoustic Doppler velocimetry, and IR imaging of the water surface. Journal of Geophysical Research-Biogeosciences 118, 770-782.

Golub, M., Desai, A.R., McKinley, G.A., Remucal, C.K., Stanley, E.H., 2017. Large Uncertainty in Estimating p
CO2
From Carbonate Equilibria in Lakes. Journal of Geophysical Research: Biogeosciences 122, 2909-2924.

Guerin, F., Abril, G., Serca, D., Delon, C., Richard, S., Delmas, R., Tremblay, A., Varfalvy, L., 2007. Gas transfer velocities of CO2 and CH4 in a tropical reservoir and its river downstream. Journal of Marine Systems 66, 161-172.

Hunt, C.W., Salisbury, J.E., Vandemark, D., 2011. Contribution of non-carbonate anions to total alkalinity and overestimation of <i>p</i>CO<sub>2</sub> in New England and New Brunswick rivers.

Biogeosciences 8, 3069-3076.

Jean-Baptiste, P., Poisson, A., 2000. Gas transfer experiment on a lake (Kerguelen Islands) using He-3 and SF6. Journal of Geophysical Research-Oceans 105, 1177-1186.

Lauerwald, R., Laruelle, G.G., Hartmann, J., Ciais, P., Regnier, P.A.G., 2015. Spatial patterns in CO2 evasion from the global river network. Global Biogeochemical Cycles 29, 534-554.

Lewis, E., Wallace, D., Allison, L.J., 1998. Program developed for CO{sub 2} system calculations. ; Brookhaven National Lab., Dept. of Applied Science, Upton, NY (United States); Oak Ridge National Lab., Carbon Dioxide Information Analysis Center, TN (United States), p. Medium: ED; Size: 40 p.

Li, S., Bush, R.T., 2015. Revision of methane and carbon dioxide emissions from inland waters in India. Global Change Biology 21, 6-8.

Li, S., Bush, R.T., Ward, N.J., Sullivan, L.A., Dong, F., 2016. Air-water CO2 outgassing in the Lower Lakes (Alexandrina and Albert, Australia) following a millennium drought. Science of the Total Environment 542, 453-468.

Li, S., Gu, S., Tan, X., Zhang, Q., 2009. Water quality in the upper Han River basin, China: The impacts of land use/land cover in riparian buffer zone. Journal of Hazardous Materials 165, 317-324.

Li, S., Ni, M., Mao, R., Bush, R.T., 2018. Riverine CO2 supersaturation and outgassing in a subtropical monsoonal mountainous area (Three Gorges Reservoir Region) of China. Journal of Hydrology 558, 460-469.

Li, S., Wang, F., Luo, W., Wang, Y., Deng, B., 2017. Carbon dioxide emissions from the Three Gorges Reservoir, China. Acta Geochimica https://doi.org/10.1007/s11631-017-0154-6

Li, S.Y., Lu, X.X., Bush, R.T., 2013. CO2 partial pressure and CO2 emission in the Lower Mekong River. Journal of Hydrology 504, 40-56.

Li, S.Y., Lu, X.X., He, M., Zhou, Y., Li, L., Ziegler, A.D., 2012. Daily CO2 partial pressure and CO2 outgassing in the upper Yangtze River basin: A case study of the Longchuan River, China. Journal of Hydrology 466, 141-150.

Liu, S., Lu, X.X., Xia, X., Yang, X., Ran, L., 2017. Hydrological and geomorphological control on CO2 outgassing from low-gradient large rivers: An example of the Yangtze River system. Journal of Hydrology 550, 26-41.

Liu, S., Lu, X.X., Xia, X., Zhang, S., Ran, L., Yang, X., Liu, T., 2016. Dynamic biogeochemical controls on river pCO(2) and recent changes under aggravating river impoundment: An example of the subtropical Yangtze River. Global Biogeochemical Cycles 30, 880-897.

Lorke, A., Bodmer, P., Noss, C., Alshboul, Z., Koschorreck, M., Somlai-Haase, C., Bastviken, D., Flury, S., McGinnis, D.F., Maeck, A., Mueller, D., Premke, K., 2015. Technical note: drifting versus anchored flux chambers for measuring greenhouse gas emissions from running waters. Biogeosciences 12, 7013-7024.

Mao, R., Chen, H., Li, S., 2017. Phosphorus availability as a primary control of dissolved organic carbon biodegradation in the tributaries of the Yangtze River in the Three Gorges Reservoir Region. Science of the Total Environment 574, 1472-1476.

Prytherch, J., Brooks, I.M., Crill, P.M., Thornton, B.F., Salisbury, D.J., Tjernstrom, M., Anderson, L.G., Geibel, M.C., Humborg, C., 2017. Direct determination of the air-sea CO2 gas transfer velocity in Arctic sea ice regions. Geophysical Research Letters 44, 3770-3778.

Ran, L., Li, L., Tian, M., Yang, X., Yu, R., Zhao, J., Wang, L., Lu, X.X., 2017. Riverine CO2 emissions in the Wuding River catchment on the Loess Plateau: Environmental controls and dam impoundment impact. Journal of Geophysical Research-Biogeosciences 122, 1439-1455.

Ran, L.S., Lu, X.X., Yang, H., Li, L.Y., Yu, R.H., Sun, H.G., Han, J.T., 2015. CO2 outgassing from the Yellow River network and its implications for riverine carbon cycle. Journal of Geophysical Research-Biogeosciences 120, 1334-1347.

Raymond, P.A., Cole, J.J., 2001. Gas exchange in rivers and estuaries: Choosing a gas transfer velocity. Estuaries 24, 312-317.

Raymond, P.A., Hartmann, J., Lauerwald, R., Sobek, S., McDonald, C., Hoover, M., Butman, D., Striegl, R., Mayorga, E., Humborg, C., Kortelainen, P., Duerr, H., Meybeck, M., Ciais, P., Guth, P., 2013. Global carbon dioxide emissions from inland waters. Nature 503, 355-359.

Raymond, P.A., Zappa, C.J., Butman, D., Bott, T.L., Potter, J., Mulholland, P., Laursen, A.E., Mcdowell, W.H., Newbold, D., 2012. Scaling the gas transfer velocity and hydraulic geometry in streams and small rivers. Limnology & Oceanography Fluids & Environments 2, 41–53.

Tranvik, L.J., Downing, J.A., Cotner, J.B., Loiselle, S.A., Striegl, R.G., Ballatore, T.J., Dillon, P., Finlay, K., Fortino, K., Knoll, L.B., 2009. Lakes and reservoirs as regulators of carbon cycling and climate. Limnology & Oceanography 54, 2298-2314.

Wang, F., Wang, B., Liu, C.Q., Wang, Y., Guan, J., Liu, X., Yu, Y., 2011. Carbon dioxide emission from surface water in cascade reservoirs–river system on the Maotiao River, southwest of China. Atmospheric Environment 45, 3827-3834.

Wang, X.F., He, Y.X., Yuan, X.Z., Chen, H., Peng, C.H., Zhu, Q., Yue, J.S., Ren, H.Q., Deng, W., Liu, H., 2017. pCO(2) and CO2 fluxes of the metropolitan river network in relation to the urbanization of Chongqing, China. Journal of Geophysical Research-Biogeosciences 122, 470-486.

Wanninkhof, R., 1992. RELATIONSHIP BETWEEN WIND-SPEED AND GAS-EXCHANGE OVER THE OCEAN. Journal of Geophysical Research-Oceans 97, 7373-7382.

Wanninkhof, R., Asher, W.E., Ho, D.T., Sweeney, C., McGillis, W.R., 2009. Advances in Quantifying Air-Sea Gas Exchange and Environmental Forcing. Annual Review of Marine Science 1, 213-244.

Wanninkhof, R., Knox, M., 1996. Chemical enhancement of CO2 exchange in natural waters. Limnology and Oceanography 41, 689-697.

Xiao, S., Yang, H., Liu, D., Zhang, C., Lei, D., Wang, Y., Peng, F., Li, Y., Wang, C., Li, X., Wu, G., Liu, L., 2014. Gas transfer velocities of methane and carbon dioxide in a subtropical shallow pond. Tellus Series B-Chemical and Physical Meteorology 66.

Yang, L., Lu, F., Wang, X., Duan, X., Tong, L., Ouyang, Z., Li, H., 2013. Spatial and seasonal variability of CO2 flux at the air-water interface of the Three Gorges Reservoir. Journal of Environmental Sciences 25, 2229-2238.

Yao, G.R., Gao, Q.Z., Wang, Z.G., Huang, X.K., He, T., Zhang, Y.L., Jiao, S.L., Ding, J., 2007. Dynamics Of CO2 partial pressure and CO2 outgassing in the lower reaches of the Xijiang River, a subtropical monsoon river in China. Science of the Total Environment 376, 255-266.

Zhang, J., Li, S., Dong, R., Jiang, C., 2018. Physical evolution of the Three Gorges Reservoir using advanced SVM on Landsat images and SRTM DEM data. Environmental Science and Pollution Research 25, 14911-14918.

Zhang, T., Li, J., Pu, J., Martin, J.B., Khadka, M.B., Wu, F., Li, L., Jiang, F., Huang, S., Yuan, D., 2017. River sequesters atmospheric carbon and limits the CO2 degassing in karst area, southwest China. Science of The Total Environment 609, 92-101.

**Table 1**. Statistics of all the data from three river systems (separated statistics please refer to Figs. S2 and S3 in the Supplementary material)s.

| | | Water T ($^0$C) | pH | Alkalinity (μeq/l) | $p$CO$_2$ (μatm) | DO% | DOC (mg/L) | TDN (mg/L) | TDP (μg/L) |
|---|---|---|---|---|---|---|---|---|---|
| Number | | 115 | 115 | 115 | 115 | 56 | 114 | 114 | 113 |
| Mean | | 22.5 | 8.39 | 2589.1 | 846.4 | 91.5 | 6.67 | 2.42 | 65.9 |
| Median | | 22.8 | 8.46 | 2560 | 588.4 | 88.8 | 2.51 | 1.56 | 50.7 |
| Std. Deviation | | 6.3 | 0.29 | 640.7 | 818.5 | 8.7 | 7.62 | 2.38 | 56.3 |
| Minimum | | 11.7 | 7.47 | 600 | 50.1 | 79.9 | 0.33 | 0.01 | 5.0 |
| Maximum | | 34 | 9.38 | 4488 | 4830.4 | 115.9 | 37.48 | 10.54 | 298.5 |
| Percentiles | 25 | 16.3 | 8.24 | 2240 | 389.8 | 84.0 | 1.33 | 0.62 | 25.1 |
| | 75 | 29 | 8.56 | 2920 | 920.4 | 99.1 | 9.96 | 3.61 | 88.1 |
| 95% CI for Mean | Lower Bound | 21.4 | 8.33 | 2470.8 | 695.2 | 89.1 | 5.26 | 1.98 | 55.4 |
| | Upper Bound | 23.7 | 8.44 | 2707.5 | 997.6 | 93.8 | 8.09 | 2.86 | 76.4 |

CI-Confidence Interval.

**Table 2.** Comparison of different model for $CO_2$ areal flux estimation using combined data (unit is mmol/m$^2$/d for $CO_2$ areal flux and cm/h for $k_{600}$).

| $CO_2$ areal flux[a] | | From FC | Flow velocity-based model (Fig. 43b) | Water depth-based model (Fig.3a) | Alin's model |
|---|---|---|---|---|---|
| $k_{600}$ | | 48.4[b] | 116.5[c] | 38.3 | 37.6 |
| Mean | | 198.1 | 476.7 | 156.6 | 154.0 |
| S.D. | | 185.5 | 446.2 | 146.6 | 144.2 |
| 95% CI for Mean | Lower Bound | 129.5 | 311.5 | 102.3 | 100.6 |
| | Upper Bound | 266.8 | 641.8 | 210.8 | 207.4 |

CI-Confidence Interval

a-$CO_2$ areal flux is based on TBL model.

b-mean level that is determined using floating chambers (FC).

c-This figure is revised to be 49.6 cm/h if the model ($k_{600}$ = 62.879FV + 6.8357, $R^2$= 0.52, p=0.019) is used (Fig. 43c), and the corresponding $CO_2$ areal flux is 203±190 mmol/m$^2$/d.

**Table 3.** $CO_2$ emission from total rivers sampled in the study.

(a) Upscaling using $CO_2$ areal flux by FC.

| | Catchment Area $km^2$ | Water surface $km^2$ | $CO_2$ areal flux mmol/$m^2$/d | $CO_2$ emission Tg $CO_2$/y |
|---|---|---|---|---|
| Daning | 4200 | 21.42 | 122.0 ±239.4 | 0.042 |
| Qijiang | 4400 | 30.8 | 50.3 ±177.2 | 0.025 |
| TGR river | 50000 | 377.78 | 217.7 ±334.7 | 1.321 |
| Total | | | | 1.39 |

(b) Upscaling using determined $k_{600}$ average and models (whole dataset are used here).

| | | From determined $k_{600}$ mean | Flow velocity-based model (Fig. 4~~3~~b) (numbers in bracket is from the revised model; Fig. 4~~3~~c) | Water depth-based model (Fig. 4~~3~~a) | Alin's model |
|---|---|---|---|---|---|
| Mean | | 1.37 | 3.29 (1.40) | 1.08 | 1.06 |
| S.D. | | 1.28 | 3.08 (1.31) | 1.01 | 1.00 |
| 95% CI for Mean | Lower Bound | 0.89 | 2.15 (0.91) | 0.71 | 0.69 |
| | Upper Bound | 1.84 | 4.43 (1.81) | 1.46 | 1.43 |

A total water area of approx. 430 $km^2$ for all tributaries (water area is from Landsat ETM+ in 2015).

带格式的：下标

带格式的：下标

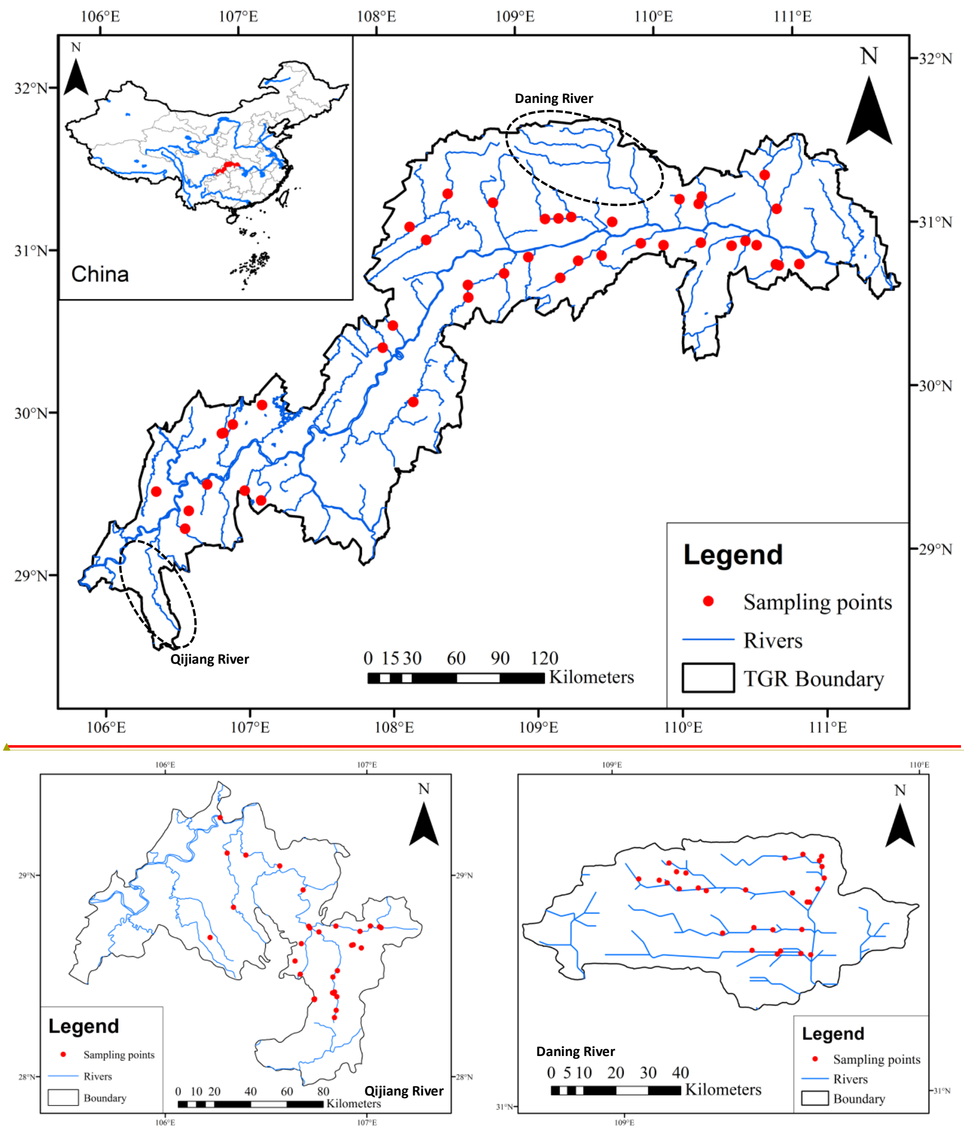


**Fig. 1.** Map of sampling locations of major rivers and streams in the Three Gorges Reservoir region, China.



带格式的：字体颜色：文字 1

带格式的：字体：小四，加粗，字体颜色：文字 1

带格式的：字体：小四，加粗，字体颜色：文字 1

带格式的：字体：(默认) Times New Roman

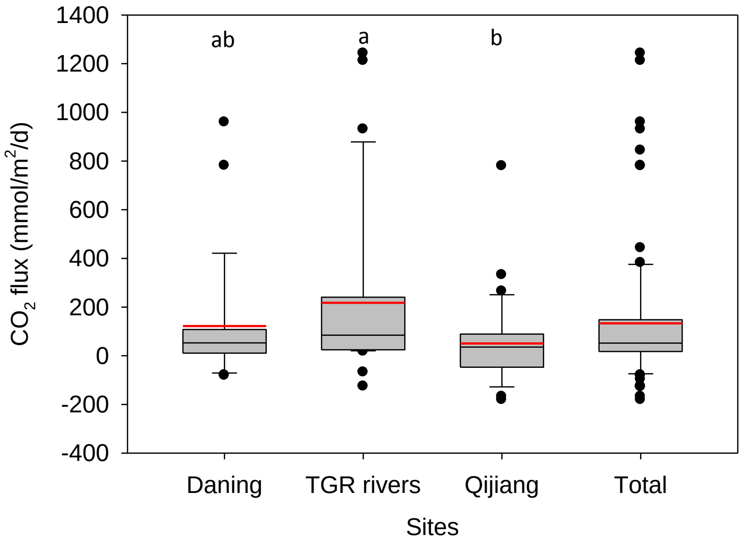


**Fig. 21.** Boxplots of $CO_2$ emission rates by floating chambers in the investigated three river systemssubtropical rivers (different letters represent statistical differences at $p<0.05$ by **Mann-Whitney Rank Sum Test**). (the black and red lines, lower and upper edges, bars and dots in or outside the boxes demonstrate median and mean values, 25th and 75th, 5th and 95th, and <5th and >95$^{th}$ percentiles of all data, respectively). (For interpretation of the references to color in this figure legend, the reader is referred to the web version of this article) (Total means combined data from three river systems).

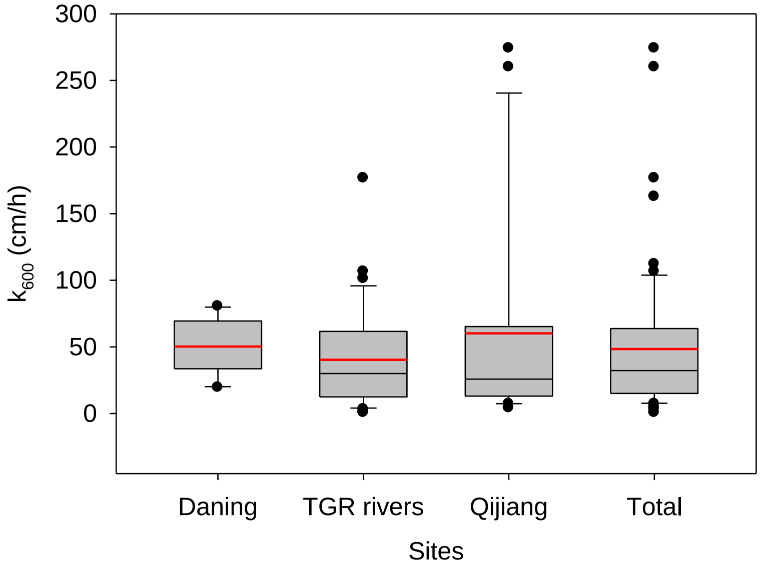


**Fig. 3~~2~~.** Boxplots of $k_{600}$ levels in the investigated three river systems~~subtropical rivers~~ (there is not a statistically significant difference in k among sites by Mann-Whitney Rank Sum Test). (the black and red lines, lower and upper edges, bars and dots in or outside the boxes demonstrate median and mean values, 25th and 75th, 5th and 95th, and <5th and >95$^{th}$ percentiles of all data, respectively). (For interpretation of the references to color in this figure legend, the reader is referred to the web version of this article) (Total means combined data from three river systems).

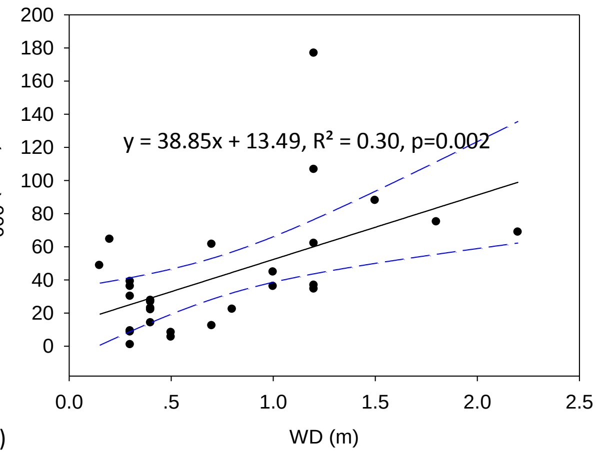


(a)

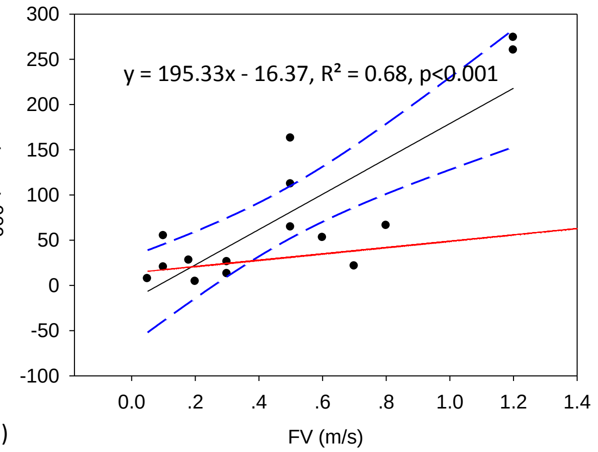


(b)

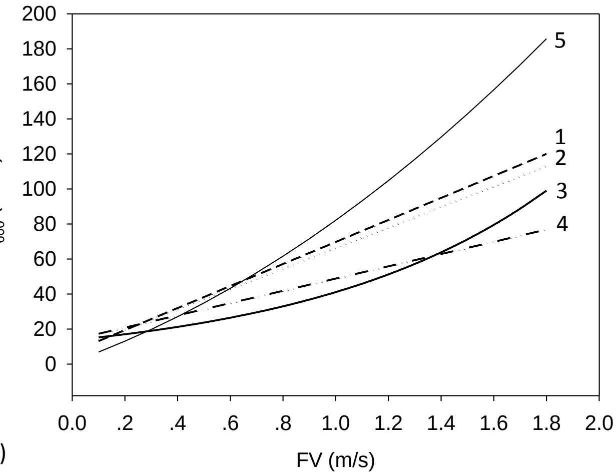


(c)

**Fig. 4~~3~~.** The $k_{600}$ as a function of water depth (WD) using data from~~in~~ TGR rivers (a), flow velocity (FV) using data from ~~in~~ Qijiang (b), and comparison of the developed model with other models (c) (others without significant relationships between k and physical factors are not shown). The solid lines show regression, the dashed lines represent 95% confidence band, and the red dash-dotted line represents the model developed by Alin et al (2011) (~~in panel b,~~ if several extremely values are removed in panel b, the revised model would be $k_{600}$ = 62.879FV + 6.8357, $R^2$ = 0.52, p=0.019) (in panel c, 1-the revised model, 2-model from Ran et al., 2017, 3-model from Ran et al., 2015, 4-model from Alin et al,, 2011, 5-model from Liu et al., 2017) (1- $k_{600}$ = 62.879FV + 6.8357; 2- $k_{600}$ = 58.47FV+7.99; 3- $k_{600}$ = 13.677exp (1.1FV); 4- $k_{600}$ = 35 FV + 13.82; 5- $k_{600}$ = 6.5FV$^2$ + 12.9FV+0.3) (unit of k in models 1-4 is cm/h, and unit of m/d for model 5 is transferred to cm/h).